Spatial solitons in chiral media

Carlos G. Avendaño and J. Adrian Reyes
Instituto de Fisica, Universidad Nacional Autónoma de México, Apartado Postal 20-364 01000, Mexico, Distrito Federal, Mexico
(Received 26 April 2004; revised manuscript received 26 July 2004; published 2 December 2004)

We study theoretically the nonlinear propagation of a narrow optical wave packet through a cholesteric liquid crystal. We derive the equations governing the weakly nonlinear dynamics of an optical field by taking into account the coupling with the liquid crystal. We constructed the solution as the superposition of four narrow wave packets centered around the linear eigenmodes of the helical structure whose corresponding envelopes A are slowly varying functions of their arguments. We found a system of four coupled equations to describe the resulting vector wave packet which has some integration constants and that under special conditions reduces to the nonlinear Schrödinger equation with space-dependent coefficients. We solved this equation both, using a variational approach and performing numerical calculations. We calculated analytically the soliton spatial scales, the transported power, the nonlinear refraction index, and its wavelength dependence, showing that this has its maxima at the edges of the reflection band. We also exhibit the existence of some other exact but non-self-focused solutions.

DOI: 10.1103/PhysRevE.70.061701 PACS number(s): 42.70.Df, 42.65.Tg, 77.84.Nh

I. INTRODUCTION

In the last decade there has been great attention to the nonlinear optics of nematic liquid crystals because of the giant optical nonlinearity of these materials—a factor of 6–10 orders of magnitude larger [1] than that of doped glasses—and the strong nonlinear effects [2] which can be achieved in nematic liquid crystals by using lasers with moderate intensity (KW/cm^2). Pioneering experiments [3] for continuous beams showed the presence of steady spatial patterns for cylindrical [3] and planar [4] geometries. The basic mechanism that governs these time-independent patterns is the balance between the nonlinear refraction (self-focusing) and the spatial diffraction of the nematic liquid crystal. A study of these experiments using separation of scales [5,6] shows that the field amplitude at the center of a Gaussian beam (inner solution) follows a nonlocal nonlinear Schrödinger (NLS) equation, which is able to describe the undulation and filamentation observed in the experiments. Some more recent work reported the observation and modeling of solitons with arbitrary nonlocality in planar nematic liquid crystal cells [7].

A different phenomenon is the propagation of wave packets, instead of continuous beams. In this case there exists the possibility of stable and robust solitary wave solutions (optical solitons), when the equilibrium between dispersion and self-focusing is reached. This possibility for planar [8] and cylindrical [9] waveguides with and without dissipation in a specific configuration has been previously considered.

Other interesting liquid crystal phases are cholesteric which due to their peculiar optical properties have been the object of intense research during more than one century [10]. Moreover, exact solutions for the electromagnetic axial propagation were found by Kats [11] and Nityananda [12], which exhibit the presence of a frequency gap in which two of the four eigenwaves are evanescent. Linear electromagnetic propagation in these structures has been much studied in the literature on either finite or infinite samples. In particular, in recent years helical structures with defects have been considered because they present a defect mode which accumulates the energy around its defect plane and might be useful in designing low threshold lasers [13]. Even though the energy accumulation around this defect implies a large optical field, nonlinear optical studies of cholesterics have been scarcely considered [14] so far in the literature.

The aim of this paper is to derive the nonlinear equation governing the structure of a spatial optical wave packet propagating axially in a cholesteric liquid crystal without dissipation. The outline of this paper is as follows. In Sec. II we state the governing coupled equations for the interaction between the electromagnetic field and the cholesteric liquid crystal. In Sec. III we restrict our model to the weakly nonlinear limit and deduce the amplitude equation for a vector wave packet whose components are narrow wave packets centered around the linear eigenmodes of the helical structure. In Sec. IV we show that the analogs of the two first conserved quantities of the nonlinear Schrödinger equation are satisfied as well as some others coming from a Lagrangian formulation. In Sec. V we show that there exist various particular solutions showing no self-focusing and found that under certain condition we obtain the nonlinear Schrödinger equation with spatially dependent coefficients. We solve it both numerically by using a variation of the split step method and analytically by using the variational approximation. We find analytically the soliton spatial scales, the transported power, the nonlinear refraction index, and its wavelength dependence. We close our paper by summarizing our work. We also include three appendixes where we (a) define all the quantities involved for writing Maxwell's equation in the Marcuvitz Schwinger representation, (b) write the explicit expression in matrix form for the well known linear solution for the helical structure, and (c) calculate the matrices involved in the vector amplitude equation we derived here.

II. BASIC EQUATIONS

Let us consider a cholesteric liquid crystal cell of thickness L whose symmetry axis is perpendicular to the cell plates as shown in Fig. 1. We restrict the director's field to the x-y plane as given by $\hat{n}(\theta(z))=(\cos\theta(z),\sin\theta(z),0)$. In the absence of external fields the equilibrium configuration is determined by the minimum of the Helmholtz free energy for cholesterics given by [15]

$$F_c=\frac{1}{2}\int [K_1(\nabla\cdot\hat{n})^2+K_2(\hat{n}\cdot\nabla\times\hat{n}+q)^2 + K_3(\hat{n}\times\nabla\times\hat{n})^2]dV, \quad (1)$$

where K_1, K_2, K_3 are the elastic constants and q is the chirality of the medium.

It is well known that F_c is minimized by a configuration described by $\theta(z)=qz$, with $q=2\pi/p$ and p the pitch or spatial period of the cholesteric helical structure.

If we propagate electromagnetic fields $\overline{E}$ and $\overline{H}$ through the cell, we have to add to F_c the electromagnetic energy density $-\frac{1}{2}\mathrm{Re}\{\overline{E}\cdot\overline{D}^*+\overline{B}\cdot\overline{H}^*\}$ which takes into account the interaction of these fields with the liquid crystal. It allow us to write the total free energy density as

$$\begin{aligned}F&=F_c-\frac{1}{2}\int \mathrm{Re}\{\overline{E}\cdot\overline{D}^*+\overline{B}\cdot\overline{H}^*\}dV\\&=\frac{1}{2}\int\Big[K_1(\nabla\cdot\hat{n})^2+K_2(\hat{n}\cdot\nabla\times\hat{n}+q)^2\\&\quad+K_3(\hat{n}\times\nabla\times\hat{n})^2-\frac{1}{2}\varepsilon_0(\varepsilon_\perp|\overline{E}|^2+\varepsilon_a|\hat{n}\,.\,\overline{E}|^2)\\&\quad-\frac{1}{2}\mu_0(\mu_\perp|\overline{H}|^2+\mu_a|\hat{n}\,.\,\overline{H}|^2)\Big]dV. \quad (2)\end{aligned}$$

Here ε_0 and μ_0 are the dielectric permittivity and magnetic permeability of the vacuum, respectively. In writing Eq. (2) we have assumed that the medium follows the magnetic and dielectric constitutive relations

$$\overline{D}=\varepsilon_0\overline{\varepsilon}\cdot\overline{E},\quad \overline{B}=\mu_0\overline{\mu}\cdot\overline{H}, \quad (3)$$

characterized by the uniaxial dielectric and magnetic tensors

$$\overline{\varepsilon}=\varepsilon_\perp\delta_{ij}+\varepsilon_a\hat{n}\hat{n}, \quad (4)$$

$$\overline{\mu}=\mu_\perp\delta_{ij}+\mu_a\hat{n}\hat{n}. \quad (5)$$

Here $\varepsilon_\perp$ and $\mu_\perp$ denote the dielectric permittivity and magnetic susceptibility perpendicular to the nematic axis and $\varepsilon_a=\varepsilon_\parallel-\varepsilon_\perp$ and $\mu_a=\mu_\parallel-\mu_\perp$ are the dielectric and magnetic anisotropies of the medium, respectively.

It is well known that the thermal fluctuations in $\hat{n}$ induce scattering of the optical field. To overcome this effect by decreasing the correlation length in $\hat{n}$, it is convenient to apply an additional low frequency electric field perpendicular to the helix axis. The intensity of this latter field should be much smaller than the critical value for untwisting the cholesteric [15]. Here, we will not consider the effect of the extra field by adding its corresponding contribution to the free energy but only by replacing the cholesteric pitch p by that obtained after distorting the helix by this field.

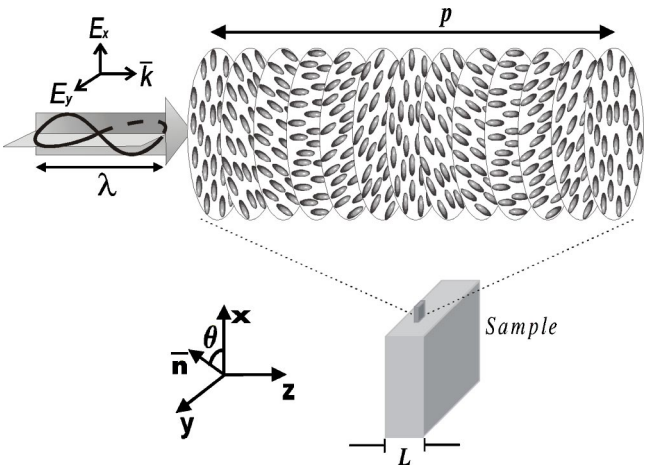

FIG. 1. A laser beam of wavelength λ propagates in a sample of chiral material of width L and spatial period p. Here we consider a beam propagating in the axial direction. $\hat{n}$ represents the average orientation of the molecules in each plane perpendicular to the axis z.

The presence of strong enough optical fields modifies the helical structure. The new equilibrium configuration is obtained by minimizing the total free energy F given by Eq. (2); it yields

$$\begin{aligned}\frac{\partial^2\theta}{\partial\zeta^2}&=-\frac{1}{q^2}\left(\frac{\partial^2\theta}{\partial x^2}+\frac{\partial^2\theta}{\partial y^2}\right)+\frac{\sigma^2}{2}\varepsilon_a[(|e_x|^2-|e_y|^2)\sin 2\theta\\&\quad-(e_x^*e_y+e_y^*e_x)\cos 2\theta]+\frac{\sigma^2}{2}\mu_a[(|h_x|^2-|h_y|^2)\sin 2\theta\\&\quad-(h_x^*h_y+h_y^*h_x)\cos 2\theta], \quad (6)\end{aligned}$$

where we used the approximation of equal elastic constants $K_1=K_2=K_3=K$ and we have written the fields in terms of the dimensionless variables

$$\overline{e}\equiv\frac{\overline{\mathcal{E}}}{e_0}\equiv\frac{Z_0^{-1/2}\overline{E}}{e_0},\quad \overline{d}\equiv\frac{\overline{\mathcal{D}}}{e_0}\equiv\frac{Z_0^{-1/2}\overline{D}}{\varepsilon_0 e_0},$$

$$\overline{h}\equiv\frac{\overline{\mathcal{H}}}{e_0}\equiv\frac{Z_0^{+1/2}\overline{H}}{e_0},\quad \overline{b}\equiv\frac{\overline{\mathcal{B}}}{e_0}\equiv\frac{Z_0^{+1/2}\overline{B}}{\mu_0 e_0}, \quad (7)$$

with $e_0\equiv Z_0^{-1/2}E_0$, E_0 the amplitude of the initial beam, and $Z_0=\sqrt{\mu_0/\varepsilon_0}$, $c=1/\sqrt{\varepsilon_0\mu_0}$ the impedance and speed of light in free space. $\zeta\equiv qz$ and $\sigma^2\equiv e_0^2/(2cKq^2)$ is a dimensionless parameter which is equal to the ratio between the electric field energy density and the elastic energy density of the cholesteric; that is to say, it is a measure of the coupling between the optical field and the cholesteric. In obtaining Eq. (6) we have assumed transverse fields, namely, $\overline{e}=(e_x(x,y,z,t),e_y(x,y,z,t),0)$ and $\overline{h}=(h_x(x,y,z,t),h_y(x,y,z,t),0)$. It is worth stressing that by taking both transverse components of the electromagnetic fields nonvanishing, we are tacitly excluding the case for which the field is perpendicular to the director and avoiding in turn a possible

first order configurational transition (Fréedericksz transition). In this way, we are not only getting rid of a threshold field but also turning around a reorientation bistability. It is therefore necessary to have a beam which impinges the cholesteric sample obliquely to the anchoring direction and to the low frequency stabilizing electric field.

Here, we restrict ourselves to analyze only the weakly nonlinear limit (Kerr medium). This implies that $\sigma \ll 1$ which amounts to requiring an optical energy density much smaller than the elastic energy density so that we can solve Eq. (6) by successive approximations in σ^2. This can be accomplished by assuming that

$$\theta(\zeta) = \theta^{(0)}(\zeta) + \sigma^2 \theta^{(1)}(\zeta) + \sigma^4 \theta^{(2)}(\zeta) + \cdots \tag{8}$$

where the zeroth order approximation $\theta^{(0)}(\zeta) = \zeta$ is corrected by the successive orders $\sigma^2\theta^{(1)}(\zeta)$, $\sigma^4\theta^{(2)}(\zeta)$,.... Notice on the one hand that by solving iteratively Eq. (9) with $\theta^{(0)}$ a ζ-dependent function we find corrections $\theta^{(1)}$, $\theta^{(2)}$,..., which have the same dependence. Hence, by assuming small configuration distortions we retain the layered structure or one dependence of the cholesteric helix. On the other hand, if $\sigma \ll 1$ the presence of the powers of σ implies that the contribution of the higher order terms is smaller than the dominant term. Thus, in the weakly nonlinear regime, we can keep the approximation (8) up to first order in σ. Interaction between the optical field and the reorientation in the liquid crystal stronger than the weakly nonlinear limit gives rise to different hierarchies of partial differential equations of higher order. Such a system has been studied previously for a nematic fiber [16]. In that case, the analysis allows the authors to derive a complex modified Korteweg–de Vries equation whose solutions are doubled embedded solitons describing ultrafast pulses.

By inserting this expression in Eq. (6) we find the following differential equation that satisfies $\theta^{(1)}(\zeta)$:

$$\frac{d^2\theta^{(1)}(\zeta)}{d\zeta^2} = \frac{1}{2}\varepsilon_a[(|e_x|^2 - |e_y|^2)\sin 2\zeta - (e_x^* e_y + e_y^* e_x)\cos 2\zeta] + \frac{1}{2}\mu_a[(|h_x|^2 - |h_y|^2)\sin 2\zeta - (h_x^* h_y + h_y^* h_x)\cos 2\zeta], \tag{9}$$

which leads to

$$\theta^{(1)}(\zeta) = -\frac{1}{8}\varepsilon_a[(|e_x|^2 - |e_y|^2)\sin 2\zeta - (e_x^* e_y + e_y^* e_x)\cos 2\zeta] - \frac{1}{8}\mu_a[(|h_x|^2 - |h_y|^2)\sin 2\zeta - (h_x^* h_y + h_y^* h_x)\cos 2\zeta] + B\zeta + C, \tag{10}$$

where B and C are integration constants.

Let us assume that the cholesteric is to satisfy hard anchoring boundary conditions at both plates given by $\theta(z=0) = \theta(z=L) = 0$. This can be valid only if the cholesteric slab contains an integer number m of spatial periods such that $qL = 2m\pi$. Hence $B = 0$ and C is completely determined so that the solution of Eq. (6) up to first order can be written as

$$\theta(z) \approx \theta^{(0)}(z) + \sigma'^2\theta^{(1)}(z) = qz + \sigma'^2 f(z) \tag{11}$$

where $\sigma'^2 \equiv \sigma^2/8$ and

$$f(z) \equiv \varepsilon_a[(|e_y|^2 - |e_x|^2)\sin 2qz + (e_x^* e_y + e_y^* e_x)(\cos 2qz - 1)] + \mu_a[(|h_x|^2 - |h_y|^2)\sin 2qz + (h_x^* h_y + h_y^* h_x) \times (\cos 2qz - 1)]. \tag{12}$$

Notice that the parameter σ'^2 is directly related to the coupling parameter σ^2; in what follows, we will take the former as the expansion parameter and to simplify notation we will suppress the prime on σ. Therefore Eq. (11) provides us the cholesteric configuration distorted by the given fields. It is convenient to express $f(z)$ as the bilinear form

$$f(z) = (e_x^*, h_x^*, e_y^*, h_y^*) \cdot M \cdot (e_x, h_x, e_y, h_y)^T, \tag{13}$$

where

$$M = \begin{pmatrix} -\varepsilon_a \sin 2qz & 0 & \varepsilon_a(\cos 2qz - 1) & 0 \\ 0 & -\mu_a \sin 2qz & 0 & \mu_a(\cos 2qz - 1) \\ \varepsilon_a(\cos 2qz - 1) & 0 & \varepsilon_a \sin 2qz & 0 \\ 0 & \mu_a(\cos 2qz - 1) & 0 & \mu_a \sin 2qz \end{pmatrix}, \tag{14}$$

Here the superscript T denotes the transpose of the involved vector or matrix.

Let us introduce a dimensionless four-component vector ψ, normalized to the initial amplitude e_0, formed by the harmonic field amplitudes $\bar{e}$ and $\bar{h}$ given by

$$(e_x, h_x, e_y, h_y)^T = \psi(\bar{r_t}, z)\exp[i(\bar{k_t} \cdot \bar{r_t} - \varpi t)], \tag{15}$$

where the subscript t refers to the transverse component of the vectors. Then we can write Maxwell's equations using the *Marcuvitz-Schwinger* representation as [17]

$$\partial_z \psi = ik_0 J_4 L \psi, \tag{16}$$

where $\partial_{ij} = \partial^2 / \partial x_i \partial x_j$ with $i, j = x, y$. Here $k_0 = \varpi / c$ is the wave number in free space, and J_4 and L are 4×4 matrices given in Appendix A. Next we derive the amplitude equation which governs a narrow wave packet.

III. AMPLITUDE EQUATION

In general the nonlinear interaction between the optical field and the cholesteric for axial propagation is governed by Eqs. (6) and (16). However, as said above, we restrict our analysis to consider only the weakly nonlinear regime. With this aim we substitute $\theta(z)$ given by Eq. (11) into Eqs. (16) and expand the result in Taylor series up to first order in σ^2. It allows us to write the matrix L in the form

$$L = \gamma_{tt} - D_t \gamma_{zz}^{-1} D_t^{\dagger}, \tag{17}$$

where

$$\gamma_{tt} \approx \gamma_{tt}^0 + \sigma^2 f(z) M_1, \tag{18}$$

$$\gamma_{tt}^0 = U^{-1} D U, \quad M_1 = \begin{pmatrix} -\varepsilon_a \sin 2qz & 0 & \varepsilon_a \cos 2qz & 0 \\ 0 & -\mu_a \sin 2qz & 0 & \mu_a \cos 2qz \\ \varepsilon_a \cos 2qz & 0 & \varepsilon_a \sin 2qz & 0 \\ 0 & \mu_a \cos 2qz & 0 & \mu_a \sin 2qz \end{pmatrix}, \tag{19}$$

$$U = \begin{pmatrix} -\sin qz & 0 & \cos qz & 0 \\ \cos qz & 0 & \sin qz & 0 \\ 0 & -\sin qz & 0 & \cos qz \\ 0 & \cos qz & 0 & \sin qz \end{pmatrix}, \tag{20}$$

$$D = \begin{pmatrix} \varepsilon_\perp & 0 & 0 & 0 \\ 0 & \varepsilon_\parallel & 0 & 0 \\ 0 & 0 & \mu_\perp & 0 \\ 0 & 0 & 0 & \mu_\parallel \end{pmatrix}. \tag{21}$$

Here we have taken advantage of the fact that for axial propagation the elements of γ_{zz}^{-1} remain constants so that the only dependence on $\hat{n}$ or $\theta(z)$ of Eq. (16) lies in the elements of the matrix γ_{tt}, in which we have inserted Eq. (11). We have also expressed explicitly γ_{tt}^0 in terms of the similarity transformation defined by the rotation U which relates γ_{tt}^0 with the diagonal matrix D. Under the above weakly nonlinear approximation Eq. (16) turns out to be

$$ik_0 J_4 \partial_z \psi + k_0^2 [U^{-1} D U + \sigma^2 f(z) M_1] \psi - k_0^2 D_t \gamma_{zz}^{-1} D_t^{\dagger} \psi = 0. \tag{22}$$

It is useful to express this equation in a system of coordinates rotating with the helix of the cholesteric for which γ_{tt} is diagonal, that is, we introduce the variable

$$\overline{\psi} = U \psi, \tag{23}$$

which after performing the derivatives and doing some simplification can be written as

$$0 = -ik_0 J_4 \partial_z \overline{\psi} - ik_0 J_4 (U \partial_z U^{-1}) \overline{\psi} + k_0^2 D \overline{\psi} + k_0^2 \sigma^2 f(z) \times (U M_1 U^{-1}) \overline{\psi} - k_0^2 (U D_t \gamma_{zz}^{-1} D_t^{\dagger} U^{-1}) \overline{\psi}. \tag{24}$$

Here we have used the identity $U J_4 U^{-1} = -J_4$ for a rotation. Notice that the last two terms account for the nonlinearity and the transverse dependence of the amplitude $\overline{\psi}$, respectively. Thus, by neglecting these two terms we restrict Eq. (24) to describing axial linear propagation, which is a problem extensively studied a long time ago [18] whose solution is analytical. Because the matrix $U \partial_z U^{-1}$ is formed by constant coefficients the linear problem can be formulated as an eigensystem whose four eigenvectors are plane waves having two different wave numbers k_i $(i = 1, 2)$ and two directions $\pm$ (see Appendix B). These modes satisfy a well known dispersion relation and two of them have a band gap for ω within $\omega_1 = qc / \sqrt{\epsilon_\parallel \mu_\parallel}$ and $\omega_2 = qc / \sqrt{\epsilon_\perp \mu_\perp}$.

If we call $T \cdot \alpha$ the matrix whose columns are these eigenvectors we can write the general solution for axial linear propagation as $\overline{\psi}_{lin} = T \cdot \alpha \cdot A^T$, where A^T is a coordinate-dependent column vector whose components are

$$A(\mathcal{X}, \mathcal{Y}, \mathcal{Z}) = (A_1^+, A_1^-, A_2^+, A_2^-). \tag{25}$$

The dimensionless amplitude A^T, which represents the envelope of a narrow wave packet of width $\kappa \equiv (k - k_0)/k_0 \ll 1$ whose central wave vector is k_0, is assumed to be a slowly varying function of its arguments $\mathcal{X} \equiv \kappa x$, $\mathcal{Y} \equiv \kappa y$, $\mathcal{Z} \equiv \kappa z$. Here κ is a small parameter that measures the statistical dispersion of the wave packet distribution in the Fourier space. In this sense the wave packet is formed by a superposition of plane waves whose wave vectors are not necessarily aligned with the z axis but constrained to a narrow cone whose axis is parallel to the same axis. Alternatively, our wave packet may also describe an incident beam showing isotropic fluctuations, in the plane perpendicular to the propagation direction, on its wave vector, if these fluctuations have a statistical dispersion κ.

We intentionally select the matching condition $\kappa = \sigma$ because it has been shown that up to $O(\sigma^3)$ this choice leads to the standard nonlinear Schrödinger equation [9,19]. It should

be pointed out that due to this matching condition, once the optical intensity has been taken, the spectral dispersion of the packet κ should assume the same value.

It is noteworthy that this model may be generalized by taking these two small expansion parameters related by $\kappa \equiv \sigma^a$, with a a positive number. Then $a=1/2$ represents a wider and $a=2$ a narrower wave packet, but only $a=1$ leads to the NLS equation for a Kerr-like medium [16]. Note that the presence of higher powers of σ implies that these higher order contributions are smaller than the dominant term, which describes a small-amplitude narrow wavepacket. Thus, the trial solution

$$\overline{\psi} = T \cdot \alpha \cdot A^T \tag{26}$$

represents the superposition of four narrow wave packets whose central wave vectors lie around those of the linear eigenvectors $T \cdot \alpha$. Then, each component of A^T is the envelope of each wave packet associated with each linear eigenmode. To simplify notation, in what follows we keep the original coordinates of A.

Here we have used the superscript $\pm$ to represent the propagation to the right and to the left of the helix and the subscripts 1, 2 to distinguish between the modes that have and do not have a band gap.

Substitution of Eq. (26) into Eq. (24) allows us to write

$$ik_0 N \cdot \partial_z B + k_0^2 N \cdot R \cdot B + k_0^2 M_t \cdot B - k_0^2 \sigma^2 f(z) M_{NL} \cdot B = 0, \tag{27}$$

where $B = \alpha \cdot A$, $f(z) = B^{*T} \cdot M \cdot B$, $M_{NL} = T^\dagger \cdot U \cdot M_1 \cdot U^{-1} \cdot T$, $M_t = T^\dagger \cdot U \cdot D_t \cdot \gamma_{zz}^{-1} \cdot D_t^\dagger \cdot U^{-1} \cdot T$, and R_{ij} is the diagonal matrix whose elements $r_i^\pm$ $(i=1,2)$ are the eigenvalues of T, that is to say,

$$R = \begin{pmatrix} r_1^+ & 0 & 0 & 0 \\ 0 & r_1^- & 0 & 0 \\ 0 & 0 & r_2^+ & 0 \\ 0 & 0 & 0 & r_2^- \end{pmatrix}. \tag{28}$$

In writing Eq. (27) we have consistently taken into account that $T \cdot \alpha$ satisfies the linear propagation equation noted above:

$$-ik_0 J_4 \partial_z (T \cdot \alpha) - ik_0 J_4 (U \partial_z U^{-1})(T \cdot \alpha) + k_0^2 D (T \cdot \alpha) = 0, \tag{29}$$

and used the following orthogonality relation:

$$T_i^\dagger \cdot J_4 \cdot T^j = N, \tag{30}$$

which was proved [20] by assuming energy conservation along the z axis. Here N is a diagonal matrix whose elements are the norms of the z component of the Poynting vector associated with each of the linear eigenvectors. However, if we previously divide each eigenmode by $\sqrt{|N_i|}$ and choose the positive (negative) sign for the waves propagating to the right (left) $A_1^\pm$, $A_2^\pm$, the matrix N takes the form

$$N = \begin{pmatrix} 1 & 0 & 0 & 0 \\ 0 & -1 & 0 & 0 \\ 0 & 0 & 1 & 0 \\ 0 & 0 & 0 & -1 \end{pmatrix}. \tag{31}$$

Equation (27) governs the nonlinear interaction among four wave packets whose central wave vectors are centered around the four existing linear eigenwaves in a cholesteric liquid crystal. Notice that it is written in terms of the 4×4 matrices M_{NL} and M_t defined in Appendix C that characterize the self-focusing or nonlinearity and the diffraction of the vector wave packet. In the next section we formulate a Lagrangian representation to obtain the conserved quantities of this vector wave packet.

IV. CONSERVED QUANTITIES

It is well known that the NLS equation satisfies an infinite hierarchy of conserved quantities. Here, for our vector amplitude equation we shall prove that the analogs to the two first conserved constants of this hierarchy are satisfied. To this end, let us multiply Eq. (27) by B^{T^*}, take the complex conjugate of the resulting expression, and subtract it from the nonconjugated expression to obtain

$$ik_0 B^{T^*} \cdot N \cdot \partial_z B + ik_0 B \cdot N \cdot \partial_z B^{T^*} + B^{T^*} \cdot k_0^2 M_t \cdot B - B \cdot k_0^2 M_t^{T^*} \cdot B^{T^*} = 0, \tag{32}$$

where we have employed the fact that $M_{NL} = M_{NL}^{T^*}$ and $f^*(z) = f(z)$ since M is also a Hermitian matrix. Integration of Eq. (32) over the whole domain of the transverse coordinates x and y leads to

$$(d/dz) \int_{-\infty}^{\infty} \int_{-\infty}^{\infty} B^{T^*} \cdot N \cdot B \, dx \, dy = 0, \tag{33}$$

which arises from the fact that M_t is also Hermitian. This can be easily shown by noting that M_t is given by $M_t = M_{L1}\partial_{xx} + M_{L2}\partial_{yy} + M_{L3}\partial_{xy}$ where M_{Lk} $(k=1,2,3)$ are in turn Hermitian matrices such that the commutators $[\partial_{ij}, M_{Lk}] = 0$ $(i,j = x,y)$ vanish. It is important to remark that Eq. (33) establishes the energy conservation along the z direction, as can be seen by recalling that the vector wave packet B was normalized to unit z component of its corresponding Poynting vector with N, given by Eq. (31), providing the sense of propagation.

To find the second integration constant, we rewrite Eq. (32) in the form

$$\begin{aligned} 0 = {} & \partial_z (B^{T^*} \cdot N \cdot B) + \partial_x \left[B^{T^*} \cdot \left(M_{L1} \partial_x + \frac{1}{2} M_{L3} \partial_y \right) B \right. \\ & \left. - B \cdot \left(M_{L1} \partial_x + \frac{1}{2} M_{L3} \partial_y \right) B^{T^*} \right] \\ & + \partial_y \left[B^{T^*} \cdot \left(M_{L2} \partial_y + \frac{1}{2} M_{L3} \partial_x \right) B \right. \\ & \left. - B \cdot \left(M_{L2} \partial_y + \frac{1}{2} M_{L3} \partial_x \right) B^{T^*} \right]. \end{aligned} \tag{34}$$

Thus, upon integration over the whole transverse domain and after using Eq. (33) we find that the current density vector $\vec{J}$ should be divergenceless:

$$\vec{J} = \int_{-\infty}^{\infty}\int_{-\infty}^{\infty}\left[B^{T*}\cdot\left(M_{L1}\partial_x + \frac{1}{2}M_{L3}\partial_y\right)B - B\cdot\left(M_{L1}\partial_x + \frac{1}{2}M_{L3}\partial_y\right)B^{T*},\right.$$

$$\left. B^{T*}\cdot\left(M_{L2}\partial_y + \frac{1}{2}M_{L3}\partial_x\right)B - B\cdot\left(M_{L2}\partial_y + \frac{1}{2}M_{L3}\partial_x\right)B^{T*}\right]dx\,dy. \quad (35)$$

That is, this current is conserved after traversing the cholesteric sample.

We can find further integration constants by calculating the Lagrangian density $\mathcal{L}$ for our system since from this we can derive conserved quantities by using the symmetries of the system and Noether's theorem [21]. We can get a Lagrangian density for Eq. (27) if we further approximate the cholesteric configuration given by Eq. (12) which strictly satisfies the hard anchoring boundary conditions. This means, by neglecting the terms arising from the integration constant C the mentioned conditions are no longer satisfied exactly, but consistently approximated in the weakly nonlinear limit. Moreover, if we are to consider cholesteric samples containing a large number of spatial periods p, ($\sim$50) the effect of this approximation on the boundary condition is almost negligible. The latter approximation amounts to replacing M by M_1 given by Eqs. (14) and (19), respectively. Hence $f(z)$ can now be expressed in the coordinate rotating system as

$$f(z) = B^{*T}(T^{\dagger}UM_1U^{-1}T)B = B^{*T}M_{NL}B. \quad (36)$$

To find the Lagrangian density of Eq. (27) it should be observed, on the one hand, that the coefficients of the two first terms are constant matrices while the coefficient of the third one (diffraction term) is only z dependent. This allows us to obtain them by taking the variational derivative of the Lagrangian density, very similar to that of the nonlinear Schrödinger equation. On the other hand, the nonlinear term of the same equation can be obtained by calculating the derivative $\partial[f(z)]^2/\partial B^T$. Therefore the corresponding Lagrangian density L_{ac} is

$$\mathcal{L}_{ac} = \frac{1}{2}ik_0(B^*\cdot N\cdot B_{,z} - B\cdot N\cdot B^*_{,z}) + k_0^2 B\cdot N\cdot R\cdot B^* - \frac{1}{2}\sigma^2k_0^2f'^2(z) - k_0^2\left(B^*_{,x}\cdot M_{L1}\cdot B_{,x} + B^*_{,y}M_{L2}B_{,y} + \frac{1}{2}B^*_{,y}M_{L3}B_{,x} + \frac{1}{2}B^*_{,x}M_{L3}B_{,y}\right), \quad (37)$$

where we have introduced the abbreviation $\partial B/\partial x_k \equiv B_{,x_k}$, $k=1,2,3$, and used the fact that $M_t = M_{L1}\partial_{xx} + M_{L2}\partial_{yy} + M_{L3}\partial_{xy}$.

Following Noether's theorem, if $d\mathcal{L}_{ac}/dx^{\alpha}=0$ then the movement constants are given by

$$T^{\alpha\beta} = \frac{\partial\mathcal{L}_{ac}}{\partial B_{\lambda,\alpha}}B_{\lambda,\beta} - \mathcal{L}_{ac}\delta_{\alpha,\beta}. \quad (38)$$

For our system $d\mathcal{L}_{ac}/dx = d\mathcal{L}_{ac}/dy = 0$ so that just the following components of $T^{\alpha\beta}$ are conserved:

$$T^{xx} = -k_0^2B^*_{,x}\cdot\left(M_{L1}B_{,x} + \frac{1}{2}M_{L3}B_{,y}\right) - k_0^2\left(B^*_{,x}M_{L1} + \frac{1}{2}B^*_{,y}M_{L3}\right)\cdot B_{,x} - L_{ac},$$

$$T^{yy} = -k_0^2B^*_{,y}\cdot\left(M_{L2}B_{,y} + \frac{1}{2}M_{L3}B_{,x}\right) - k_0^2\left(B^*_{,y}M_{L2} + \frac{1}{2}B^*_{,x}M_{L3}\right)\cdot B_{,y} - \mathcal{L}_{ac},$$

$$T^{xy} = -k_0^2B^*_{,y}\cdot\left(M_{L1}B_{,x} + \frac{1}{2}M_{L3}B_{,y}\right) - k_0^2\left(B^*_{,x}M_{L1} + \frac{1}{2}B^*_{,y}M_{L3}\right)\cdot B_{,y},$$

$$T^{yx} = -k_0^2B^*_{,x}\cdot\left(M_{L2}B_{,y} + \frac{1}{2}M_{L3}B_{,x}\right) - k_0^2\left(B^*_{,y}M_{L2} + \frac{1}{2}B^*_{,x}M_{L3}\right)\cdot B_{,x}. \quad (39)$$

After subtraction of the components T^{xx} and T^{yy}, we arrive at

$$T^{xxyy} = -k_0^2\left(M_{L1}B_{,x} + \frac{1}{2}M_{L3}B_{,y}\right)B^*_{,x} - k_0^2\left(B^*_{,x}M_{L1} + \frac{1}{2}B^*_{,y}M_{L3}\right)B_{,x} + k_0^2\left(M_{L2}B_{,y} + \frac{1}{2}M_{L3}B_{,x}\right)B^*_{,y} + k_0^2\left(B^*_{,y}M_{L2} + \frac{1}{2}B^*_{,x}M_{L3}\right)B_{,y}. \quad (40)$$

Because of its simplicity we shall use this particular movement constant to check the convergence of the numerical calculations we perform below.

V. SOME PARTICULAR SOLUTIONS

Some interesting features of the nonlinear interaction governed by Eq. (27) arise from the explicit form of M_{NL} which has a 2×2 block matrix structure with vanishing diagonal blocks. A direct consequence of this structure is that a wave packet centered around a single linear eigenmode does not have nonlinear self-focusing so that a pure wave packet which enters the sample spreads as it advances along the helix direction. The same happens when the wave packet is formed by the superposition of either the modes B_1^+ and B_1^- or B_2^+ and B_2^-, for which we combine modes traveling to the right and to the left. Hence, the nonlinear term of Eq. (27) is

nonvanishing either when we mix modes propagating in the same direction or when they have different wave numbers. Further properties of this nonlinear interaction can be derived by calculating $f(z)$, that is,

$$f(z) = i\{m_1(B_1^+B_2^{+*} - B_1^{+*}B_2^+) + m_1(B_1^-B_2^{-*} - B_1^{-*}B_2^-) + m_2(B_1^-B_2^{+*} - B_1^{-*}B_2^+) + m_2(B_1^+B_2^{-*} - B_1^{+*}B_2^-)\}. \quad (41)$$

This expression shows that $f(z)$ vanishes even though we assume the presence of the four wave packets, unless there exists a phase mismatch between two of the wave packets. This expression also shows that another spreading solution (without self-focusing) of Eq. (27) is obtained if we take the same amplitude for all the wave packets $B_1^+=B_2^+=B_1^-=B_1^+$ and the phase mismatch between the right propagating wave packets $B_1^+B_2^{+*}-B_1^{+*}B_2^+$ equal to minus that of the left propagating ones $-(B_1^-B_2^{-*}-B_1^{-*}B_2^-)$.

As a simple example of a self-focusing solution, let us restrict ourselves to considering only two propagating eigenmodes $B_2^+=\exp(i\alpha z)B_1^+$ having a phase mismatch α. If we take only one transverse coordinate amplitude, we arrive at

$$2ik_0\partial_z B_1^+ + k_0^2(n_1^+ + n_2^+ - \alpha/k_0)B_1^+ + k_0^2\eta(z)\partial_{x,x}B_1^+ - 4k_0^2m_1^2\sigma^2\sin^2(\alpha z)|B_1^+|^2B_1^+ = 0, \quad (42)$$

where

$$\eta(z) = \frac{1}{h_2}\{[c_{22}r_1^2 + c_{12}r_2^2 + 2c_{52}r_1r_2\cos(\alpha z)]\cos^2(qz) + [c_{21}r_1^2 + c_{11}r_2^2 + 2c_{51}r_1r_2\cos(\alpha z)]\sin^2(qz) + c_{53}r_1r_2\sin(\alpha z)\sin(2qz)\}. \quad (43)$$

Then, recalling that $B_1^+=A_1^+\exp(ik_0n_1^+z)$ and introducing the variable $G=A_1^+\exp[-(ik_0/2)(n_2^+-\alpha/k_0)z]$ we find the following nonlinear Schrödinger equation with spatially dependent coefficients:

$$i\partial_z G + \frac{k_0}{2}\eta(z)\partial_{x,x}G - 2k_0m_1^2\sigma^2\sin^2(\alpha z)|G|^2G = 0. \quad (44)$$

It is necessary to recall that, as said above, the amplitude G in the previous equation is dimensionless with normalization e_0.

Equation (44) can be rewritten in terms of dimensionless variables as

$$i\partial_{z'}G + \frac{1}{2}D(z')\partial_{x',x'}G - \gamma(z')|G|^2G = 0, \quad (45)$$

$$x' \equiv \frac{x}{x_0}, \quad z' \equiv \frac{z}{z_0}, \quad (46)$$

where $x'\equiv x/x_0$, $z'\equiv z/z_0$. Here x_0 and z_0 are space scales given by

$$x_0^2 \equiv \frac{1}{2k_0^2m_1^2\sigma^2}, \quad z_0 \equiv \frac{1}{2k_0m_1^2\sigma^2}, \quad (47)$$

and

$$D(z') \equiv k_0^2\eta(z'), \quad qz \to 2\pi\left(\frac{z_0}{p}\right)z', \quad \alpha z \to \alpha z_0 z', \quad (48)$$

$$\gamma(z') \equiv \sin^2(\alpha z_0 z'),$$

and the sample width is now $L'=L/z_0$. It is interesting to mention that in the case of a standard NLS equation x_0 represents the width of the optical stripe at which the self-focusing and the spatial diffraction balance each other. However, in our case there exists a longitudinal spatial dependence in the equation's coefficients which makes the width stripe oscillate with a spatial scale z_0.

Again, to simplify notation, in what follows we suppress the prime in Eq. (45).

A. Numerical solution method

The numerical procedure, called the split-step method, to solve the self-focusing $[\gamma(z)<0]$ NLS equation when its coefficients are constants is well established (see, for example, [19,22]). Here, we extend this method to consider the defocusing case $[\gamma(z)>0]$ such that both coefficients $D(z)$ and $\gamma(z)$ are z dependent. Following the original papers [23,24], the dark soliton of the NLS equation is given by the following *hyperbolic tangent* profile:

$$G(x,z) = A_0\tanh\left[\sqrt{\frac{\gamma(z)}{D(z)}}A_0x\right] + i\sqrt{1-A_0^2}, \quad (49)$$

where A_0 is an arbitrary amplitude such that the pulse width is proportional to $A_0^{-1}\sqrt{D(z)/\gamma(z)}$. Notice from this expression that the initial pulse is localized at $z=0$ whose mass center is also at $x_0=0$.

We assume the initial profile of Eq. (49) to integrate Eq. (45) numerically by using the split-step method which was performed using a lattice array whose transverse and longitudinal steps are $\Delta x=10/32$ and $\Delta z=1/8000$.

Our results were obtained by using values for a sample with pitch $p=0.29$ μm, width $L=5.2$ μm, dielectric permittivities $\epsilon_\parallel=2.62$, $\epsilon_\perp=2.31$, and elastic constant $K=5.2\times10^{-12}$ N. The cholesteric liquid crystals used were made by mixing Merck ZLI 2293 liquid crystals and ZLI 811 chiral dopants in the ratio of 2:1 [25]. We restrict our calculation to values within the visible range and outside of the band gap. It is well known that in the visible range the magnetic anisotropy μ_a is nearly equal to zero; we here take $\mu_a=0.1$.

From the third term in Eq. (44) we obtain the nonlinear refractive index n_2^{chol} as [19]

$$n_2^{chol} = \frac{\varepsilon_0m_1^2p^2}{32\pi^2K_2}. \quad (50)$$

For the parameter values given above and optical wavelength $\lambda_0=0.5$ μm, $n_2^{chol}=3.85\times10^{-23}(\mathrm{km/V})^2$, which is two orders of magnitude smaller than in nematics [$n_2^{nem}=1.43\times10^{-21}(\mathrm{km/V})^2$ [26]] but five orders larger than $n_2^{SiO_2}=1.2\times10^{-28}(\mathrm{km/V})^2$. This shows the existence of the expected giant nonlinearity for liquid crystals [1]. It also indicates how

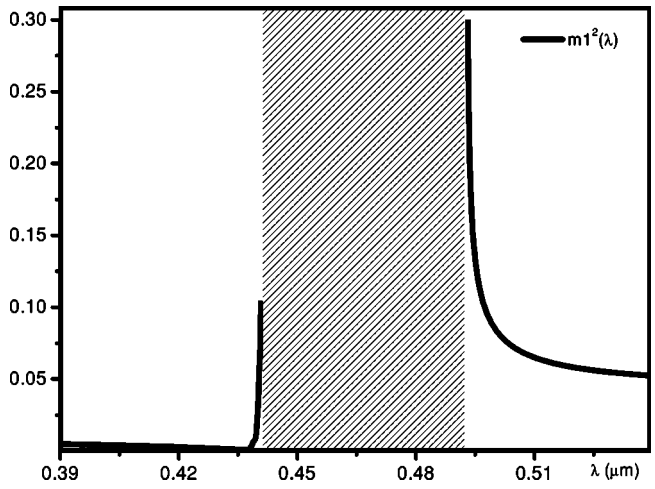

FIG. 2. Plot of dimensionless coefficient $m_1^2(\lambda)$ as a function of wavelength λ. The hatched region represents the band gap which ranges from $\lambda_{min}=0.441$ μm to $\lambda_{max}=0.492$ μm. Here $m_1^2(\lambda_v)=0$ when $\lambda_v=0.434$ μm.

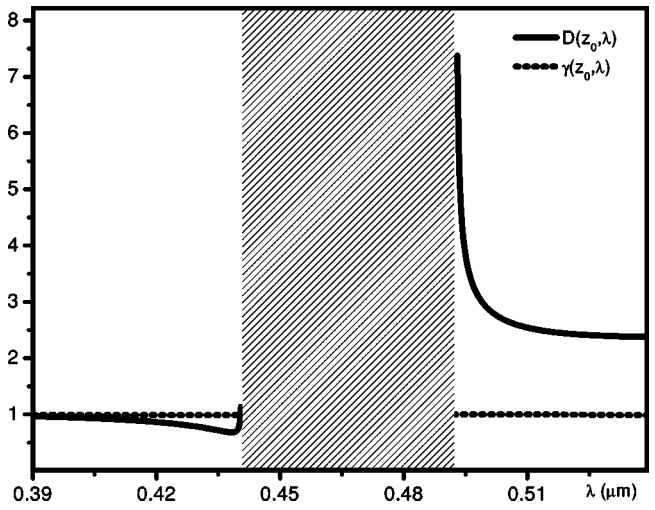

FIG. 3. Plot of dimensionless coefficients $D(z_{max},\lambda)$ and $\gamma(z_{max},\lambda)$ as functions of wavelength λ. The value of z_{max} is choosen so that $\gamma(z_{max},\lambda)$ has a maximum.

the twisted structure of the cholesteric liquid crystal, for which the elastic energy density is larger than that of nematics, does not allow one easily to distort the sample, and as a consequence its nonlinearity is smaller than that of nematics.

The nonlinear refractive index n_2^{chol} is related to the wavelength λ_0, in a nontrivial way, through the coefficient m_1^2, which is plotted in Fig. 2. As can be seen, this coefficient diverges at both band edges: $\lambda_{min}=p\sqrt{\epsilon_\perp\mu_\perp}$ and $\lambda_{max}=p\sqrt{\epsilon_\parallel\mu_\parallel}$. This fact can be shown directly by expanding $m_1^2(\lambda)$ around λ_{min} and λ_{max}. It yields

$$m_1^2(\lambda)_{\lambda\to\lambda_{min,max}} \approx \sqrt{p}\begin{cases} \varkappa_{min}(-\lambda+\lambda_{min})^{-1/2}, \\ \varkappa_{max}(\lambda-\lambda_{max})^{-1/2}, \end{cases} \tag{51}$$

where $\varkappa_{min,max}$ are given in Appendix C. To understand intuitively why the system shows these divergences, it is convenient to remark that the Poynting vector of two of the linear eigenmodes vanishes precisely at the band edges so that the energy flux is stopped there, the cholesteric distortion is the largest, and the nonlinearity as well. Strictly speaking these divergences are to be replaced by maxima if the realistic small absorption of cholesterics were taken into account. This analysis exhibits how the nonlinear effects are to be enhanced and have their largest response for the band edge wavelengths. Indeed, these results are in qualitative agreement with the mirrorless cholesteric lasing experiments [27] in which the exciting laser beam and the sample emission wavelengths almost coincide with the reflection band edges.

We should also mention that, in contrast to the enhancement of the nonlinear effects in the band edges, there exists a specific value λ_v where m_1^2 vanishes, that is to say, the nonlinearity disappears and the Eq. (44) simply transforms in a dispersion linear equation. Explicitly, $\lambda_v=p\sqrt{(\epsilon_\perp\mu_\perp\epsilon_a^2-\epsilon_\parallel\mu_\parallel\mu_a^2)/[(\epsilon_a+\mu_a)(\epsilon_a-\mu_a)]}=0.434$ μm.

An important quantity that characterizes these dark solitons is the power P_s required to generate them, which amounts to the power transported by the solitons. It can be shown that [19]

$$P_s=\frac{1}{2}\varepsilon_0 c s_0 E_0^2, \tag{52}$$

where s_0 is the transverse area of the sample and initial amplitude E_0 is related with the soliton space width x_0 through the relations (47) by

$$E_0=\frac{\lambda_0}{x_0}\sqrt{\frac{8K_2}{\varepsilon_0 m_1^2 p^2}}=\frac{\lambda_0}{2\pi x_0}\sqrt{\frac{1}{n_2^{chol}}}.$$

If we take the stripe thickness $x_0=5$ μm and $s_0=400$ μm^2, we obtain $E_0=2.56\times10^6$ V/m and hence the power is $P_s=3.48$ W, which can be produced by a laser of moderate power. We should mention that P_s is roughly one order of magnitude larger than the power used to induce spatial soliton in nematics [7]. Taking into account P_s and a beam waist 20 μm we estimate the longitudinal space length $z_0=3.1\times10^{-4}$ m which is more than one order of magnitude larger than x_0. Thus, to observe this longitudinal oscillation it would be required to have a large sample. We should recall that this is indeed a dark soliton so that these dimensions characterize a lower energy density region immersed within the path of the incident beam.

As said above, the parameter expansion σ^2 must be sufficiently small to validate our results. In effect, by substituting the previously given values we obtain $\sigma^2=0.003$. Thus, the wave packet that we are dealing with is a narrow wave packet of width $\kappa=\sqrt{\sigma^2}=0.054$ around the central wave vector k_0.

As can be noted from Eq. (45), the coefficients D and γ depend on the wavelength λ_0. Figure 3 show this dependence evaluated at one of the multiple z positions where these oscillatory co-efficients have their maxima $[z_{max}=\pi/(2\alpha z_0)]$. Notice that these coefficients are of the same order of mag-

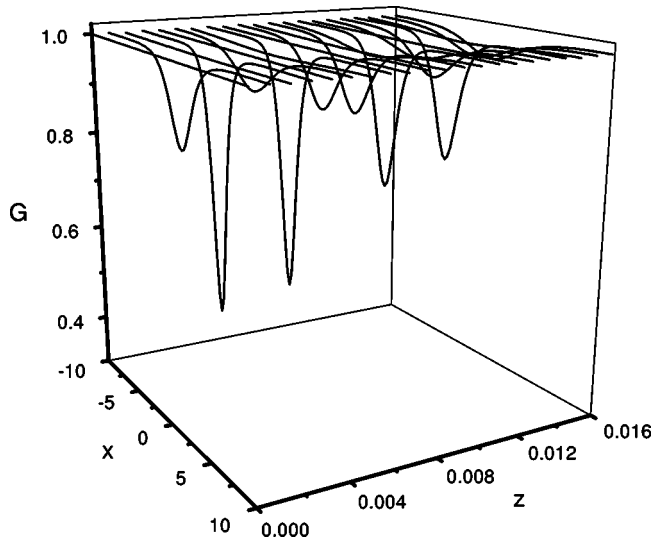

FIG. 4. The plot shows a dark soliton propagating throughout the sample of dimensionless width equal to $L/z_0=1.6\times10^{-2}$. Here we have taken amplitude $A_0=1$.

nitude in such a way that there exists a balance between self-focusing or nonlinearity and diffraction of the wave packet.

Finally, Fig. 4 shows various dark soliton profiles calculated from Eq. (45) as a function of z. As discussed above Eq. (45) predicts that each transverse profile of our solution has a different width b which oscillates with z, reaching a maximum value $b_{max}=x_0=5$ μm. Notice that, due to the balance between nonlinearity and diffraction, the average effect on the incident pulse is to maintain its hyperbolic-tangent-like profile as it extends in the z direction.

B. Variational approximation method

This formalism starts by postulating a trial analytical function or ansatz. In the case of the NLS equation a commonly adopted ansatz [24,28] that approximates a perturbed soliton is

$$G(x,z)_{ansatz} = B\tanh[F(x-x_0)] + iA,$$

$$A^2 + B^2 = 1. \tag{53}$$

The variable x represents the transverse coordinate and the parameters are allowed to be functions of the evolution variable z. B is the real amplitude, F^{-1} represents the pulse width, and x_0 is the position of the mass center. Governing equations for the evolution of free parameters can be obtained by calculating an *effective Lagrangian* L_{eff} by means of straightforward integration of the *Lagrangian density* $\mathcal{L}$ on the transverse coordinates to finally minimize L_{eff} with respect to these parameters. The solution obtained from the differential equations permit us to know the system behavior [29].

A straightforward analysis shows that a direct application of the variational formalism using the standard Lagrangian density $\mathcal{L}$ of the NLS equation $[\gamma(z)>0]$, does not work [24] so that this method should be modified, for instance, using renormalized integrals of motion [30] from which an appropriate Lagrangian density can be obtained to derive Eq. (45) for the case $D(z)=\gamma(z)=1$. Here, we consider the case in which $D(z)$ is a function of z and $\gamma(z)=cte$. Renormalizing Eq. (45) by making $G\rightarrow G\exp(-i\gamma z)$ yields

$$i\partial_z G + \frac{1}{2}D(z)\partial_{x,x}G - \gamma(|G|^2-1)G = 0, \tag{54}$$

whose appropriate Lagrangian density is

$$\mathcal{L} = \frac{i}{2}(G^*G_{,z} - GG^*_{,z})\left(1-\frac{1}{|G|^2}\right) - \frac{1}{2}D(z)|G_{,x}|^2 - \frac{1}{2}\gamma(z)(|G|^2-1)^2. \tag{55}$$

Now, substitution of $G(x,z)_{ansatz}$ into $\mathcal{L}$ and integration on the transversal coordinate $L_{eff}=\int_{-\infty}^{\infty}\mathcal{L}(G)dx$ leads us to the effective Lagrangian

$$L_{eff} = 2x_0'\left[-AB+\tan^{-1}\left(\frac{B}{A}\right)\right] - \frac{2}{3}\left(B^2FD + \frac{B^4}{F}\gamma\right). \tag{56}$$

The corresponding equations of motion may be obtained from the Euler-Lagrange equations

$$\frac{\partial L_{eff}}{\partial p_j} - \frac{d}{dz}\frac{\partial L_{eff}}{\partial p_j'} = 0, \quad p_j \equiv x_0,F,B, \quad p_j' \equiv \partial_z p_j,$$

so that we finally arrive at the following results:

$$B'(z) = 0,$$

$$x_0'(z) = \sqrt{\gamma D(z)}A(z),$$

$$F(z) = \sqrt{\frac{\gamma}{D(z)}}B(z), \tag{57}$$

which coincide with those given by the analytical solution in the case $D(z)=cte$.

As mentioned above, the pulse width is given by $F^{-1}(z) = \sqrt{[D(z)/\gamma]}B^{-1}(z)$. Taking into account that within a sample of width L there are several spatial periods p, the pulse width will show such oscillations; thus we can assume that the solution G will just be perturbed by the average of such oscillations. As a result we can use the trial solution (53) with variable parameters (57) and average values $D \equiv\langle D(z)\rangle$, $\gamma\equiv\langle\gamma(z)\rangle$,

$$D \equiv \frac{1}{2}k_0^2\left(\frac{1}{h_2}\right)[(c_{22}+c_{21})r_1^2 + (c_{12}+c_{11})r_2^2], \tag{58}$$

$$\gamma \equiv \frac{1}{2}. \tag{59}$$

After calculating the average values $D\equiv\langle D(z)\rangle$, $\gamma \equiv\langle\gamma(z)\rangle$ in Eq. (45) we arrive at the nonlinear Schrödinger equation with constant coefficients whose exact solution is given by Eq. (49). Direct comparison of both solutions

shows that the numerical and variational ones are in good agreement.

VI. SUMMARY AND PERSPECTIVES

We derived an amplitude equation for describing the weakly nonlinear interaction between the four wave packets whose central wave number is centered around those of the linear electromagnetic modes characterizing a helical structure. We showed that under certain approximations the governing amplitude equations can be derived from a Lagrangian density and calculated their conserved quantities by using their symmetries and Noether's theorem. We also showed that the analogs to the two first integrations of the hierarchy satisfying the NLS equation are satisfied by our vector wave packet.

We discussed how the nonlinear term of the envelope equation (27) is such that there exist various exact solutions which are not submitted to self-focusing. Under specific conditions of phase mismatch and amplitude relations for a two-component wave packet we derived a NLS equation with z-dependent coefficients. We found both numerically and analytically (but approximated) a dark soliton solution which has a longitudinal oscillating structure that, due to the balance between nonlinearity and diffraction, the average effect on the incident pulse is to maintain its hyperbolic-tangent-like profile as it extends in the z direction.

For the solitonlike soliton we obtained some important physical properties as such the nonlinear refractive index n_2^{chol}, which we found to be two orders of magnitude smaller than that of nematics but five orders larger than typical values for $n_2^{SiO_2}$. Hence, our result shows the existence of the-expected giant nonlinearity for liquid crystals. Additionally, we showed that this giant nonlinearity is enhanced in both edges of the band gap as a direct consequence of the fact that the Poynting vector of two of the linear eigenmodes vanishes precisely there, so that the energy flux is stopped and the cholesteric distortion is the largest as well as the nonlinearity. Qualitatively, this behavior is in agreement with the mirrorless cholesteric lasing experiments in which the exciting laser beam and the sample emission wavelengths almost coincide with the reflection band edges. Of course, our analysis was not performed to describe the interaction of the cholesteric with two beams having different frequencies like the systems reported in the mentioned experiments; however, the maxima of n_2^{chol} at the band edges makes plausible a better theoretical description which remains to be assessed.

We estimated the necessary power P to generate these dark solitons. We found that these can be generated by a laser of modest power, namely, of the order of ~ 3.5 W.

Finally, we showed that effectively we dealt with a narrow wave packet of width $\kappa = 0.054$ around the central wave vector k_0.

Our model has not take into account explicitly the unavoidable linear and nonlinear absorption effect. We have also ignored the transitory effect induced by the director reorientation and hydrodynamical coupling coming with these effects.

APPENDIX A

Maxwell's equations under the Marcuvitz-Schwinger representation Eq. (16) are written in terms of the matrices J_4 and L, which are defined as

$$J_4 = \mathrm{Kron}(J_2, J_2) = \begin{pmatrix} 0 & 0 & 0 & 1 \\ 0 & 0 & -1 & 0 \\ 0 & -1 & 0 & 0 \\ 1 & 0 & 0 & 0 \end{pmatrix}, \tag{A1}$$

$$L = \gamma_{tt} - (D_t + \Gamma_t + \gamma_{tz})\gamma_{zz}^{-1}(D_t^{\dagger} + \Gamma_t^{\dagger} + \gamma_{zt}), \tag{A2}$$

with

$$\gamma_{tt} = \begin{pmatrix} \gamma_{xx} & \gamma_{xy} \\ \gamma_{yx} & \gamma_{yy} \end{pmatrix}, \ \gamma_{tz} = \begin{pmatrix} \gamma_{xz} \\ \gamma_{yz} \end{pmatrix}, \ \gamma_{zt} = \begin{pmatrix} \gamma_{zx} & \gamma_{zy} \end{pmatrix},$$

$$D_t = (ik_0)^{-1}\mathrm{kron}(J_2\partial_t, J_2), \quad \Gamma_t = \mathrm{kron}(J_2\kappa_t, J_2),$$

$$\partial_t = \begin{pmatrix} \partial_x & \partial_y \end{pmatrix}^T, \quad \kappa_t = \begin{pmatrix} \kappa_x & \kappa_y \end{pmatrix}^T, \tag{A3}$$

$$J_2 = \begin{pmatrix} 0 & 1 \\ -1 & 0 \end{pmatrix}, \quad J_4 = J_4^{-1} = J_4^T. \tag{A4}$$

$\overline{\kappa} = \overline{k}/k_0$ is the normalized incident wave vector, the superscript † indicates the adjoint Hermitian, the elements γ_{ij} $(i,j = x,y,z)$ of γ_{tt}, γ_{zt}, γ_{tz} are the following 2×2 matrices:

$$\gamma_{ij} = \begin{pmatrix} \varepsilon_{ij} & 0 \\ 0 & \mu_{ij} \end{pmatrix}, \tag{A5}$$

and $\mathrm{Kron}(A,B)$ represents the Kronecker product with elements $a_{ij}B$. ε_{ij} and μ_{ij} represent the elements of the uniaxial dielectric and magnetic tensors shown above by Eqs. (4) and (5).

If we restrict our system to the case when the electromagnetic wave propagates in direction z through a sample of chiral material then $N_t = 0$ and $\gamma_{zt} = \gamma_{tz} = 0$. In this way the matrix L reduces to

$$L = \gamma_{tt} - D_t\gamma_{zz}^{-1}D_t^{\dagger}. \tag{A6}$$

APPENDIX B

The linear system defined by Eq. (29) which describes the linear propagation through a cholesteric liquid crystal can be expressed as $d(T\cdot\alpha)/dz = i(\omega/c)A\cdot(T\cdot\alpha)$, where $T\cdot\alpha = (\psi_1^+, \psi_1^-, \psi_2^+, \psi_2^-)$ is the matrix whose columns are the normalized eigenvectors $\psi_k^{\pm} = (e_1, e_2, h_1, h_2)$ $(k = 1,2)$ of the matrix A given by [18]

$$A = \begin{pmatrix} 0 & -i\widetilde{q} & 0 & \mu_{\perp} \\ i\widetilde{q} & 0 & -\mu_{\parallel} & 0 \\ 0 & -\epsilon_{\perp} & 0 & -i\widetilde{q} \\ \epsilon_{\parallel} & 0 & i\widetilde{q} & 0 \end{pmatrix}. \tag{B1}$$

Here e_1, e_2 and h_1, h_2 are the components of the electromagnetic vectors in a rotating frame having one of the axes x

along the optical axis; ϵ_i and μ_i are the principal values of ϵ and μ, respectively; $\tilde{q}=qc/\omega$, where $q=2\pi/p$ and p is the helix pitch. If we omit the factor $\exp(-i\omega t)$, the eigenwaves of A are $(T\cdot\alpha)_k^{\pm}=\psi_k^{\pm}\exp(i\omega n_k^{\pm}z/c)$ where

$$T=\begin{pmatrix} n_1u_1/r_1 & -n_1u_1/r_1 & n_2u_2/r_2 & -n_2u_2/r_2 \\ -4in_1\tilde{q}\epsilon/r_1 & 4in_1\tilde{q}\epsilon/r_1 & -4in_2\tilde{q}\epsilon/r_2 & 4in_2\tilde{q}\epsilon/r_2 \\ -i\tilde{q}(u_2-4\epsilon_{\parallel}\mu)/r_1 & -i\tilde{q}(u_2-4\epsilon_{\parallel}\mu)/r_1 & -i\tilde{q}(u_1-4\epsilon_{\parallel}\mu)/r_2 & -i\tilde{q}(u_1-4\epsilon_{\parallel}\mu)/r_2 \\ (4\tilde{q}^2\epsilon+u_1\epsilon_{\parallel})/r_1 & (4\tilde{q}^2\epsilon+u_1\epsilon_{\parallel})/r_1 & (4\tilde{q}^2\epsilon+u_2\epsilon_{\parallel})/r_2 & (4\tilde{q}^2\epsilon+u_2\epsilon_{\parallel})/r_2 \end{pmatrix}, \tag{B2}$$

$$\alpha=\begin{pmatrix} \exp(ik_0n_1^{+}z) & 0 & 0 & 0 \\ 0 & \exp(ik_0n_1^{-}z) & 0 & 0 \\ 0 & 0 & \exp(ik_0n_2^{+}z) & 0 \\ 0 & 0 & 0 & \exp(ik_0n_2^{-}z) \end{pmatrix}, \tag{B3}$$

and $\omega n_k^{\pm}/c$ $(k=1,2)$ are the corresponding eigenvalues given by

$$n_k^{+2}=-n_k^{-}=a_1+\tilde{q}^2+(-)^k u/2. \tag{B4}$$

In Eq. (B2) we have used the notation $u\equiv\sqrt{4a_2\tilde{q}^2+\epsilon_c^2}$, $u_1\equiv -u+\epsilon_c$, $u_2\equiv u+\epsilon_c$, $a_1\equiv(\epsilon_{\parallel}\mu_{\perp}+\epsilon_{\perp}\mu_{\parallel})/2$, $a_2\equiv 2a_1+\epsilon_{\parallel}\mu_{\parallel}+\epsilon_{\perp}\mu_{\perp}$, and $\epsilon_c\equiv\epsilon_{\parallel}\mu_{\perp}-\epsilon_{\perp}\mu_{\parallel}$, $\epsilon\equiv(\epsilon_{\parallel}+\epsilon_{\perp})/2$, $\mu=(\mu_{\parallel}+\mu_{\perp})/2$. Each eigenvector of A appearing in the columns of T, Eq. (B2), is normalized such that the z component of the Poynting vector is unity. Thus, the corresponding norms are

$$r_k\equiv\sqrt{\psi_k^{\pm}J_4\psi_k^{\pm *}}=\sqrt{2n_k[u_k^2\epsilon_{\parallel}+4\tilde{q}^2\epsilon(u_k-u_{2,1}+4\epsilon_{\parallel}\mu)]},$$

$$k=1,2.$$

Notice that for real ϵ_i and μ_i, n^2 is real according to Eqs. (B4), and the wave vectors k_0n are real or purely imaginary. Only the modes $1^{\pm}$ show a band gap for ω within $\omega_1<\varpi<\omega_2$, where $\omega_1=qc/\sqrt{\epsilon_{\parallel}\mu_{\parallel}}$, $\omega_2=qc/\sqrt{\epsilon_{\perp}\mu_{\perp}}$.

APPENDIX C

Here we find explicit expressions for the matrices M_t and M_{NL} involved in the vector envelope equation given by Eq. (27). By inserting U, T, M_1, and D_t from Eqs. (20), (B2), (19), and (A3) into expressions $M_t=T^{\dagger}\cdot U\cdot D_t\cdot\gamma_{zz}^{-1}\cdot D_t^{\dagger}\cdot U^{-1}\cdot T$ and $M_{NL}=T^{\dagger}\cdot U\cdot M_1\cdot U^{-1}\cdot T$, we arrive at

$$M_t=M_{L1}\partial_{xx}+M_{L2}\partial_{yy}+M_{L3}\partial_{xy}, \tag{C1}$$

where the Hermitian matrices M_{L1}, M_{L2}, and M_{L3} are defined by

$$M_{L1}=\begin{pmatrix} F_{11} & F_{13} & F_{15} & F_{16} \\ F_{13} & F_{11} & F_{16} & F_{15} \\ F_{15}^{*} & F_{16}^{*} & F_{12} & F_{14} \\ F_{16}^{*} & F_{15}^{*} & F_{14} & F_{12} \end{pmatrix},$$

$$M_{L2}=\begin{pmatrix} F_{21} & F_{23} & F_{25} & F_{26} \\ F_{23} & F_{21} & F_{26} & F_{25} \\ F_{25}^{*} & F_{26}^{*} & F_{22} & F_{24} \\ F_{26}^{*} & F_{25}^{*} & F_{24} & F_{22} \end{pmatrix}, \tag{C2}$$

$$M_{L3}=\begin{pmatrix} F_{31} & F_{33} & F_{35} & F_{36} \\ F_{33} & F_{31} & F_{36} & F_{35} \\ F_{35}^{*} & F_{36}^{*} & F_{32} & F_{34} \\ F_{36}^{*} & F_{35}^{*} & F_{34} & F_{32} \end{pmatrix}, \quad \text{and}$$

$$M_{NL}=i\begin{pmatrix} 0 & 0 & -m_1 & -m_2 \\ 0 & 0 & -m_2 & -m_1 \\ m_1 & m_2 & 0 & 0 \\ m_2 & m_1 & 0 & 0 \end{pmatrix}, \tag{C3}$$

Here the components m_i and F_{ij} of these matrices are given by

$$m_{1,2}\equiv\frac{\tilde{q}(u_1-u_2)\{\pm 4n_1n_2\epsilon\epsilon_a+[4\tilde{q}^2\epsilon+\epsilon_{\parallel}(u_1+u_2-4\epsilon_{\parallel}\mu)]\mu_a\}}{r_1r_2},$$

$$F_{1j}\equiv\frac{(c_{j2}\cos^2 qz+c_{j1}\sin^2 qz)}{h}, \tag{C4}$$

$$F_{2j}\equiv\frac{(c_{j1}\cos^2 qz+c_{j2}\sin^2 qz)}{h}, \quad j=1,2,3,4,$$

$$F_{3j}\equiv\frac{(c_{j3}\cos qz\sin qz)}{h}, \tag{C5}$$

$$F_{1k}\equiv\frac{c_{k2}\cos^2 qz+c_{k1}\sin^2 qz-ic_{k3}\cos qz\sin qz}{h_3},$$

$$F_{2k} \equiv \frac{c_{k1}\cos^2 qz + c_{k2}\sin^2 qz + ic_{k3}\cos qz \sin qz}{h_3}, \quad k = 5,6,$$

$$F_{3k} \equiv \frac{c_{k4}\cos qz \sin qz - ic_{k3}(\sin^2 qz - \cos^2 qz)}{h_3} \quad \text{(C6)}$$

with

$$c_{(1,2)1} \equiv 16n_{1,2}^2\tilde{q}^2\epsilon^2\epsilon_\perp + (4\tilde{q}^2\epsilon + u_{1,2}\epsilon_\parallel)\mu_\perp,$$

$$c_{(1,2)2} \equiv n_{1,2}^2 u_{1,2}^2\epsilon_\perp + \tilde{q}^2(u_{2,1} - 4\epsilon_\parallel\mu)^2\mu_\perp,$$

$$c_{(1,2)3} \equiv 2n_{1,2}^2(u_{1,2}^2 - 16\tilde{q}^2\epsilon^2)\epsilon_\perp - 2[16\tilde{q}^4\epsilon^2 + u_{1,2}^2\epsilon_\parallel^2 - \tilde{q}^2(u_{2,1}^2 - 8u_{1,2}\epsilon\epsilon_\parallel - 8u_{2,1}\epsilon_\parallel\mu + 16\epsilon_\parallel^2\mu^2)]\mu_\perp,$$

$$c_{(3,4)1} \equiv -16n_{1,2}^2\tilde{q}^2\epsilon^2\epsilon_\perp + (4\tilde{q}^2\epsilon + u_{1,2}\epsilon_\parallel)\mu_\perp,$$

$$c_{(3,4)2} \equiv -n_{1,2}^2 u_{1,2}^2\epsilon_\perp + \tilde{q}^2(u_{2,1} - 4\epsilon_\parallel\mu)^2\mu_\perp,$$

$$c_{(3,4)3} \equiv -2n_{1,2}^2(u_{1,2}^2 - 16\tilde{q}^2\epsilon^2)\epsilon_\perp - 2[16\tilde{q}^4\epsilon^2 + u_{1,2}^2\epsilon_\parallel^2 - \tilde{q}^2(u_{2,1}^2 - 8u_{1,2}\epsilon\epsilon_\parallel - 8u_{2,1}\epsilon_\parallel\mu + 16\epsilon_\parallel^2\mu^2)]\mu_\perp,$$

$$c_{(5,6)1} \equiv \pm 16n_1n_2\tilde{q}^2\epsilon^2\epsilon_\perp + (4\tilde{q}^2\epsilon + u_1\epsilon_\parallel)(4\tilde{q}^2\epsilon + u_2\epsilon_\parallel)\mu_\perp,$$

$$c_{(5,6)2} \equiv \pm n_1n_2u_1u_2\epsilon_\perp + \tilde{q}^2(u_1 - 4\epsilon_\parallel\mu)(u_2 - 4\epsilon_\parallel\mu)\mu_\perp,$$

$$c_{(5,6)3} \equiv \tilde{q}^2(u_1 - u_2)\{\pm 4n_1n_2\epsilon\epsilon_\perp + [4\tilde{q}^2\epsilon + \epsilon\|(u_1 + u_2 - 4\epsilon_\parallel\mu)]\mu_\perp,$$

$$c_{(5,6)4} \equiv \pm 2n_1n_2(u_1u_2 - 16\tilde{q}^2\epsilon^2)\epsilon_\perp - 2(16\tilde{q}^4\epsilon^2 + u_1u_2\epsilon_\parallel^2)\mu_\perp - 2\tilde{q}^2\{4\epsilon_\parallel[-4\epsilon_\parallel\mu^2 + u_2(\epsilon + \mu)] + u_1[-u_2 + 4\epsilon_\parallel(\epsilon + \mu)]\}\mu_\perp, \quad \text{(C7)}$$

$$h = \begin{cases} h_1 \text{ if } j \text{ odd}, \\ h_2 \text{ if } j \text{ even}, \end{cases}$$

$$h_1 \equiv k_0^2 r_1^2\epsilon_\perp\mu_\perp, \quad h_2 \equiv k_0^2 r_2^2\epsilon_\perp\mu_\perp, \quad h_3 \equiv k_0^2 r_1 r_2\epsilon_\perp\mu_\perp, \quad \text{(C8)}$$

$$\varkappa_{\min} = \frac{(\epsilon_\parallel\mu_\parallel - \epsilon_\perp\mu_\perp)^{1/2}}{(\epsilon_\perp\mu_\perp)^{1/4}}\frac{\mu_a^2}{t^2}(\epsilon_\perp\mu_\perp - \epsilon_\parallel\mu_\parallel)(a_1 + \epsilon_\perp\mu_\perp),$$

$$\varkappa_{\max} = \frac{(\epsilon_\parallel\mu_\parallel - \epsilon_\perp\mu_\perp)^{1/2}}{(\epsilon_\parallel\mu_\parallel)^{1/4}}\frac{\epsilon_\parallel^2\epsilon_a^2}{2^{5/2}\epsilon^2},$$

where $t = 2^{5/4}\{2\epsilon_\perp\mu^2 + \epsilon\mu_\perp[\epsilon_\parallel\mu_\parallel - \epsilon_\perp(\mu_\perp + 2\mu)]\}^{1/2}$.

[1] N. V. Tabiryan, A. V. Sukhov, and B. Ya. Zeldovich, Mol. Cryst. Liq. Cryst. **136**, 1 (1986); I. C. Khoo, Prog. Opt. **26**, 108 (1988).
[2] I. C. Khoo, H. Li, Appl. Phys. B: Lasers Opt. **59**, 573 (1994).
[3] E. Braun, L. P. Faucheux, A. Libchaber, D. W. McLaughlin, D. J. Muraki, and M. J. Shelley, Europhys. Lett. **23**, 239 (1993).
[4] E. Braun, L. P. Faucheux, and A. Libchaber, Phys. Rev. A **48**, 611 (1993).
[5] D. W. McLaughlin, D. J. Muraki, M. J. Muraki, M. J. Shelley, and X. Wang, Physica D **88**, 55 (1995).
[6] D. W. McLaughlin, D. J. Muraki, and M. J. Shelley, Physica D **97**, 471 (1996).
[7] C. Conti *et al.*, Phys. Rev. Lett. **91**, 073901 (2003); G. Assanto and M. Peccianti, IEEE J. Quantum Electron. **39**, 13 (2003).
[8] R. F. Rodríguez and J. A. Reyes, J. Mol. Liq. **71**, 115 (1997).
[9] J. A. Reyes and R. F. Rodríguez, Phys. Rev. E **65**, 051701 (2002); R. F. Rodríguez and J. A. Reyes, Opt. Commun. **197**, 103 (2001); J. A. Reyes and R. F. Rodríguez, Physica D **141**, 333 (2000).
[10] K. Robbie, D. J. Broer, and M. J. Brett, Nature (London) **399**, 764 (1999).
[11] E. I. Kats, Sov. Phys. JETP **32**, 1004 (1971).
[12] R. Nityananda, Mol. Cryst. Liq. Cryst. **21**, 315 (1973).
[13] J. Schmidtke, W. Stille, and H. Finkelmann, Phys. Rev. Lett. **90**, 083902 (2003).
[14] S. K. Srivatsa and G. S. Ranganath, Opt. Commun. **180**, 349 (2000).
[15] P. G. De Gennes, *The Physics of Liquid Crystals* (Clarendon, Oxford, 1974).
[16] R. F. Rodríguez, J. A. Reyes, A. Espinosa-Cerón, J. Fujioka, and B. Malhomed, Phys. Rev. E **68**, 036606 (2003).
[17] N. Marcuvitz and J. Schwinger, J. Appl. Phys. **22**, 806 (1951).
[18] M. Becchi, S. Ponti, J. A. Reyes, and C. Oldano, Phys. Rev. B **70**, 033103 (2004).
[19] A. C. Newell, *Nonlinear Optics* (Addison-Wesley, Reading, CA, 1992).
[20] C. Oldano, Phys. Rev. A **40**, 6014 (1989).
[21] Herbert Goldstein, *Classical Mechanics* (Addison-Wesley, Reading, MA, 1980).
[22] F. D. Tappert and C. N. Judice, Phys. Rev. Lett. **29**, 1308 (1972).
[23] V. E. Zakharov and A. B. Shabat, Sov. Phys. JETP **37**, 823 (1973).
[24] Y. S. Kivshar and V. Królikovski, Opt. Commun. **114**, 353 (1995).
[25] Min-Hyong Lee, Young-Chol Yang, Jac-Eun Kim, and Hae Yong Park, Phys. Rev. E **68**, 051701 (2003).
[26] J. A. Reyes and P. Palffy-Muhoray, Phys. Rev. E **58**, 5855 (1998).
[27] A. Muñoz, P. Palffy-Muhoray, and B. Taheri, Opt. Lett. **26**, 804 (2001); E. Alvarez *et al.*, Mol. Cryst. Liq. Cryst. Sci. Technol., Sect. A **369**, 75 (2001).
[28] P. Öhberg and L. Santos, J. Phys. B **34**, 4721 (2001).
[29] D. Anderson, Phys. Rev. A **27**, 3135 (1983).
[30] Yu. S. Kivshar and X. Yang, Phys. Rev. E **49**, 1657 (1994).